Composite Dielectric Waveguides

EIKICHI YAMASHITA, SENIOR MEMBER, IEEE, KAZUHIKO ATSUKI, AND RYOJI KUZUYA

Abstract—**Composite dielectric waveguides, or a class of dielectric waveguides made of a few dielectric materials, are described. A composite circular dielectric waveguide (CCDW) is treated with the the point-matching method. Computed values of the propagation constant of the CCDW are compared with those of the homogeneous circular dielectric waveguides (HCDW). Microwave experiments carried out to confirm the theory are described.**

I. Introduction

THE HOMOGENEOUS circular dielectric waveguide has been well investigated by many researchers since the study by Hondros and Debye in 1910 [1]. Besides, various types of dielectric waveguides have recently been tested in the field of millimeter wave circuits [2], and optics [3].

Two interesting features have been found in the dominant propagation mode of the homogeneous circular dielectric waveguide; the nonexistence of cutoff frequency and a degeneracy of two independent polarizations. Polarization instability due to inevitable waveguide imperfections makes it hard to construct a polarization-dependent transmission line. Boundary deformation of the waveguide [4] serves to separate the polarization degeneracy. The exposed cladding technique proposed by Ramaswamy *et al.* [5] is another method for the same purpose in the case of optical fibers. Composite dielectric waveguide structures are found to be also useful to separate the polarization degeneracy.

Composite dielectric waveguides, or dielectric rod structures composed of a few dielectric materials, are expected to be applicable for millimeter wave and optical transmission. This paper describes the modal analysis of a composite circular dielectric waveguide as a typical structure of this class, and microwave experiments to confirm the theory.

II. Method of Analysis

Fig. 1 shows a class of composite dielectric waveguides which could be analyzed by the present method. A circular composite dielectric waveguide shown in Fig. 2 is analyzed here as a typical structure by expanding the point-matching method discussed in an earlier paper [4].

At first, we pay attention to the z component of the electric field and magnetic field vector. Such components

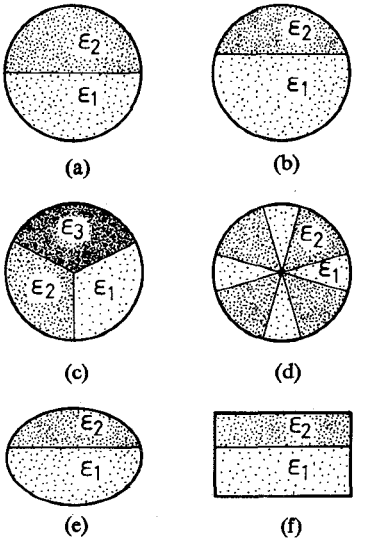

Fig. 1. Cross sections of various composite dielectric waveguides.

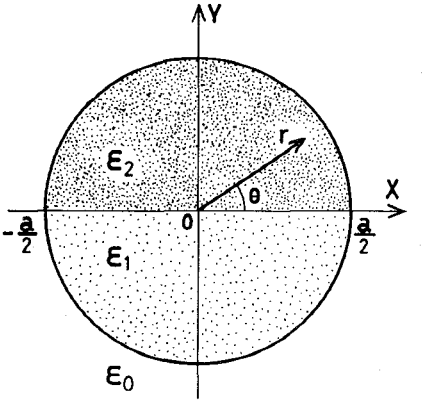

Fig. 2. The cross section of a composite circular dielectric waveguide.

must satisfy the wave equations

$$(\nabla^2+k^2)\begin{Bmatrix} E_z \\ H_z \end{Bmatrix}=0 \tag{1}$$

and boundary conditions.

When the propagation factor, $\exp(j\omega t-j\beta z)$, is assumed in the field functions, E_z and H_z, and the circular cylindrical coordinates are employed, the wave equations are written as

$$\left(\frac{\partial^2}{\partial r^2}+\frac{1}{r}\frac{\partial}{\partial r}+\frac{1}{r^2}\frac{\partial^2}{\partial \theta^2}-\beta^2+k^2\right)\begin{Bmatrix} E_z \\ H_z \end{Bmatrix}=0. \tag{2}$$

Manuscript received February 22, 1980; revised April 30, 1980.

The authors are with University of Electro-Communications, Chofu-shi, Tokyo, Japan 182.

0018-9480/80/0900-0986$00.75 ©1980 IEEE

Because we have three dielectric regions as shown in Fig. 2, the wavenumber k has different values in each region as

$$k_0^2=\omega^2\epsilon_0\mu_0 \tag{3-a}$$

$$k_1^2=\omega^2\epsilon_1\mu_0 \tag{3-b}$$

$$k_2^2=\omega^2\epsilon_2\mu_0. \tag{3-c}$$

The propagation constant β should be in the range of

$$k_0<\beta<k_1 \tag{4-a}$$

or

$$k_1<\beta<k_2. \tag{4-b}$$

Therefore, we newly define h_0, h_1, and h_2, as

$$h_0^2\equiv\beta^2-k_0^2 \tag{5-a}$$

$$h_1^2\equiv\begin{cases}\beta^2-k_1^2, & k_1<\beta<k_2\\ k_1^2-\beta^2, & k_0<\beta<k_1\end{cases} \tag{5-b}$$

$$h_2^2\equiv k_2^2-\beta^2 \tag{5-c}$$

and derive three types of general solutions for (2), namely,

$$E_{zi}=\sum_{n=0}^{\infty}\left[A_{ni}\sin(n\theta)+B_{ni}\cos(n\theta)\right]\cdot F_{ni}(h_ir)\exp(j\omega t-j\beta z),\quad i=0,1,2 \tag{6-a}$$

$$H_{zi}=\sum_{n=0}^{\infty}\left[C_{ni}\sin(n\theta)+D_{ni}\cos(n\theta)\right]\cdot F_{ni}(h_ir)\exp(j\omega t-j\beta z),\quad i=0,1,2 \tag{6-b}$$

where the subscript i corresponds to the dielectric region, 0, 1, or 2.

The functions expressed by $F_{ni}(h_ir)$ are the Bessel function or modified Bessel function depending on h_i. Because $F_{ni}(h_ir)$ must be finite at $r=0$ or $r=\infty$, the following functions are given for $F_{ni}(h_ir)$:

$$F_{n0}(h_0r)=K_n(h_0r) \tag{7-a}$$

$$F_{n1}(h_1r)=\begin{cases}I_n(h_1r), & k_1<\beta<k_2\\ J_n(h_1r), & k_0<\beta<k_1\end{cases} \tag{7-b}$$

$$F_{n2}(h_2r)=J_n(h_2r) \tag{7-c}$$

where $K_n(h_0r)$ is the modified Bessel function of second kind, $I_n(h_1r)$ the modified Bessel function of first kind, and $J_n(h_2r)$ the Bessel function of first kind.

Transverse components of the electromagnetic fields can be derived by using the above functions and Maxwell's equations, namely,

$$E_r=\frac{-j\beta}{k^2-\beta^2}\left[\frac{\partial E_z}{\partial r}+\frac{\omega\mu_0}{\beta r}\frac{\partial H_z}{\partial\theta}\right] \tag{8-a}$$

$$E_\theta=\frac{-j\beta}{k^2-\beta^2}\left[\frac{1}{r}\frac{\partial E_z}{\partial\theta}-\frac{\omega\mu_0}{\beta}\frac{\partial H_z}{\partial r}\right] \tag{8-b}$$

$$H_r=\frac{-j\beta}{k^2-\beta^2}\left[-\frac{k^2}{\omega\mu_0\beta r}\frac{\partial E_z}{\partial\theta}+\frac{\partial H_z}{\partial r}\right] \tag{8-c}$$

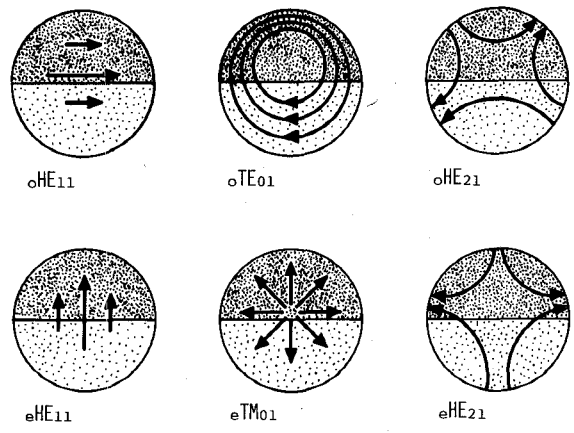

Fig. 3. Conceptual electric field distributions of the composite circular dielectric waveguide.

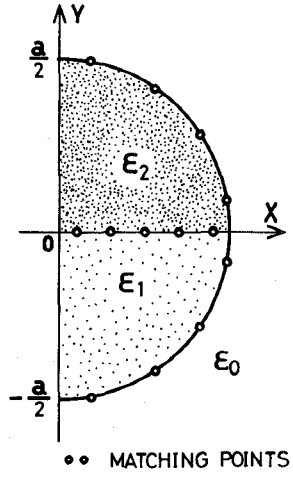

Fig. 4. The boundary surface taken in the analysis. These matching points correspond to the case of $N=9$.

$$H_\theta=\frac{-j\beta}{k^2-\beta^2}\left[\frac{k^2}{\omega\mu_0\beta}\frac{\partial E_z}{\partial r}+\frac{1}{r}\frac{\partial H_z}{\partial\theta}\right] \tag{8-d}$$

in each dielectric region.

Tangential components at any point on the dielectric interface can be expressed by combining the r and θ components of the fields at the point. The interface conditions imposed on field functions are the continuation of these tangential components.

The direct application of the interface condition to (6-a) and (6-b) would not lead to any solution because these are made of infinite series. To make the problem tractable, the interface conditions are satisfied by finite series only at a finite number of points on the boundary. This procedure is called the point-matching method as discussed in [4] and [6]. A proper choice of boundary points makes a set of homogeneous linear equations concerning A_{ni}, B_{ni}, C_{ni}, and D_{ni}. The determinant of these linear equations should vanish to obtain nontrivial solutions. The solution of the determinantal equation gives the propagation constant in a similar fashion to [4].

Fig. 3 illustrates the electric field distribution in the composite circular dielectric waveguide in Fig. 2. At pre-

TABLE I
THE CONVERGENCE PROPERTY OF β/k_0 FOR AN INCREASING N;
$\epsilon_1^*=2.04$, $\epsilon_2^*=2.53$, $k_0a=9.0$.

N	$_oHE_{11}$	$_eHE_{11}$	$_oTE_{01}$	$_eTM_{01}$	$_oHE_{21}$	$_eHE_{21}$
5	1.473	-	1.340	-	1.272	-
7	1.473	1.461	1.352	1.337	1.272	1.294
9	1.472	1.463	1.357	1.337	1.300	1.293
11	1.472	1.462	1.357	1.337	1.300	1.293
13	1.472	1.462	1.357	1.337	1.300	1.293

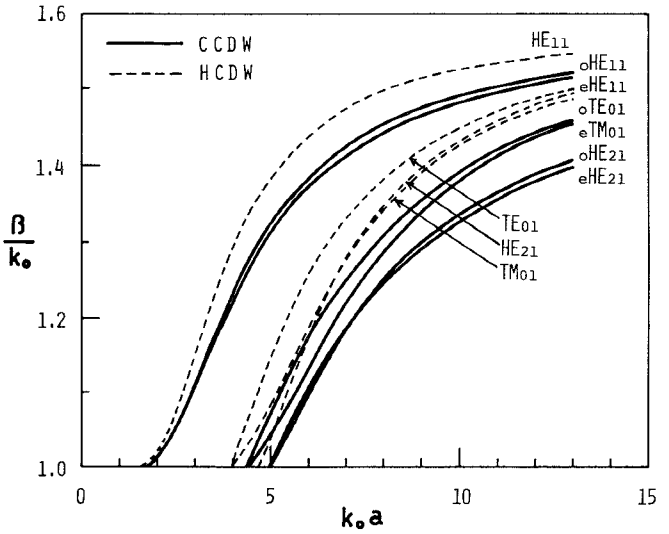

Fig. 5. Computed values of β/k_0 for a composite circular dielectric waveguide (CCDW) made of Teflon ($\epsilon_1^*=2.04$) and Rexolite ($\epsilon_2^*=2.53$), and for a homogeneous circular dielectric waveguide (HCDW) made of Rexolite.

sent, any symbols to identify the propagation modes of this waveguide have not been known, so that we employ similar symbols to the homogeneous circular dielectric waveguide. The suffix o and e have added to these designations which mean an odd and even symmetry, respectively.

Fig. 4 shows a half of the waveguide structure that is considered in the analysis because of symmetry.

III. NUMERICAL RESULTS

The determinantal equation derived by truncating (6-a) and (6-b) and by imposing the interface conditions was numerically solved on an electronic computer HITAC-8800.

When N terms are taken in (6-a) and (6-b), the number of matching points are selected as $N-1$ on the boundary

$$r=\frac{a}{2} \qquad -\frac{\pi}{2}\leqslant\theta\leqslant\frac{\pi}{2} \tag{9-a}$$

and $(N+1)/2$ on the boundary

$$\theta=0 \qquad 0\leqslant r\leqslant\frac{a}{2} \tag{9-b}$$

The case of $N=9$, for example, is illustrated in Fig. 4. After all, a determinantal equation is given and β/k_0 is computed.

Teflon ($\epsilon_1^*=2.04$) and Rexolite ($\epsilon_2^*=2.53$) were employed as two materials of the composite circular dielectric waveguide. Table I shows the computed values of β/k_0 for six propagation modes. These results are thought to indicate reasonable convergence for an increasing N.

Fig. 5 shows the computed values of β/k_0 as a function of k_0a for various lower order modes. It is obvious that the HE_{11} mode of the circular Rexolite-rod waveguide shown as a dotted line is separated to the oHE_{11} mode and eHE_{11} mode of the composite circular dielectric waveguide. The HE_{21} mode is also separated to the oHE_{21} mode and eHE_{21} mode. Furthermore, the TE_{01} mode and TM_{01} mode are changed to the oTE_{01} mode and eTM_{01} mode, respectively. The oTE_{01} mode and eTM_{01} mode are not complete transverse modes but hybrid modes.

It is also possible to judge which dielectric material confines more electromagnetic energy only by looking at the value of β/k_0. For example, the value of β/k_0 for the HE_{11} mode in Fig. 5 is closer to that of the oHE_{11} mode than that of the eHE_{11} mode, so that the energy of the oHE_{11} mode is more confined in Rexolite than in Teflon compared with the eHE_{11} mode.

Figs. 6, 7, and 8 show the computed values of β/k_0 for three different modes of the composite circular dielectric waveguide with various compositions of dielectric materials.

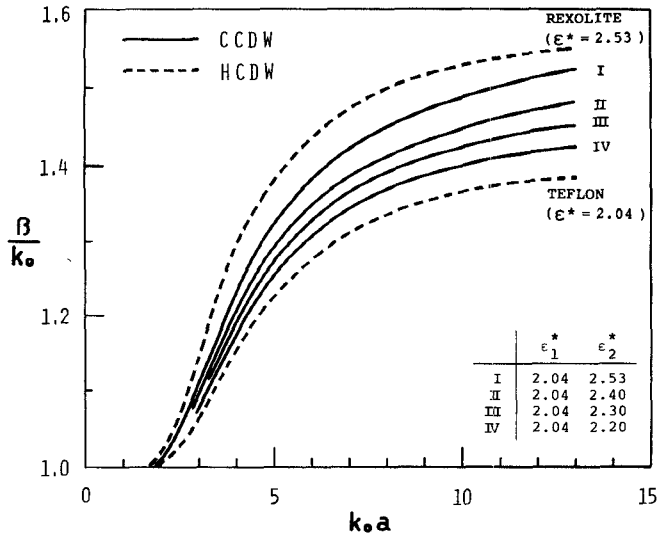

Fig. 6. Computed values of β/k_0 of the $o\mathrm{HE}_{11}$ mode for various combinations of dielectric materials.

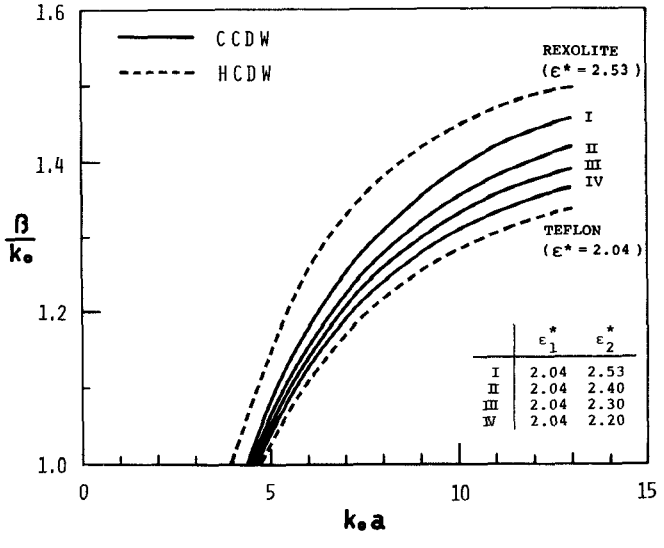

Fig. 7. Computed values of β/k_0 of the $o\mathrm{HE}_{01}$ mode for various combinations of dielectric materials.

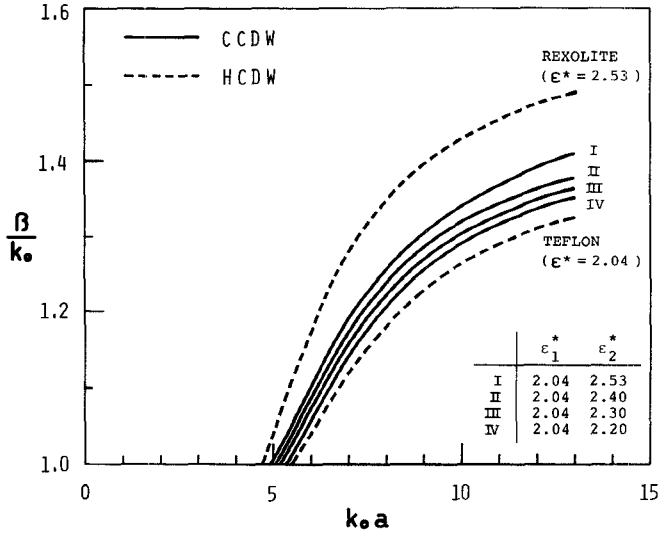

Fig. 8. Computed values of β/k_0 of the $o\mathrm{HE}_{21}$ mode for various combinations of dielectric materials.

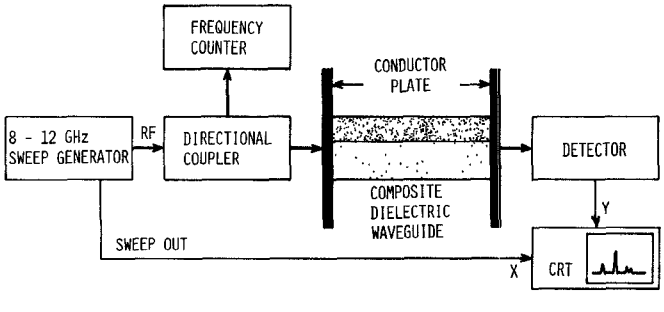

Fig. 9. Microwave measurement setup of the propagation constant.

IV. Microwave Experiments

Microwave experiments concerning the propagation constant of a composite circular dielectric waveguide of Teflon and Rexolite were carried out by using a measurement setup as shown in Fig. 9. Two semicircular dielectric rods of 10 cm in length and 1~4 cm in diameter were fixed with adhesive paste to form a composite dielectric waveguide. The waveguide was placed between two con-

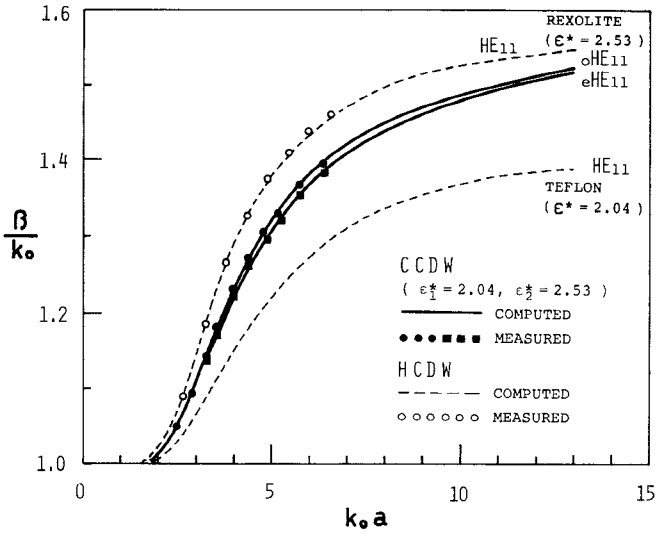

Fig. 10. Computed and measured values of β/k_0 for the $o\mathrm{HE}_{11}$ and $e\mathrm{HE}_{11}$ modes.

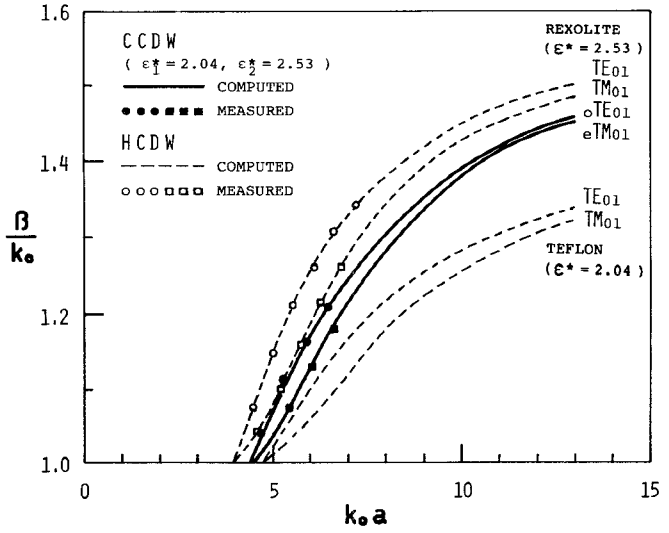

Fig. 11. Computed and measured values of β/k_0 for the $o\mathrm{TE}_{01}$ and $e\mathrm{TM}_{01}$ modes.

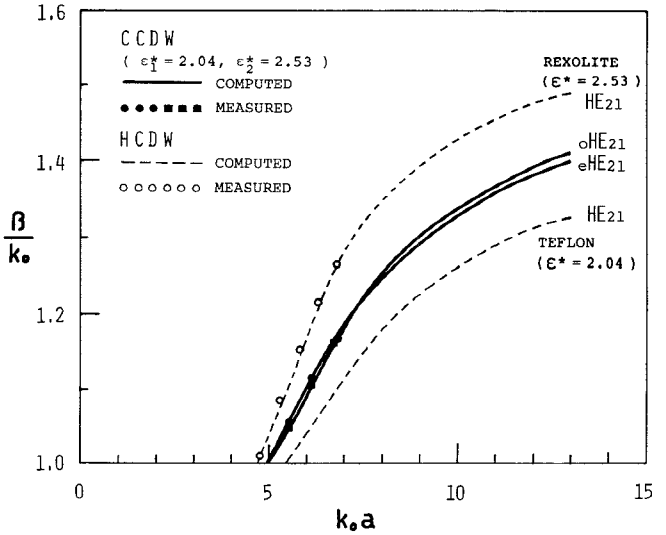

Fig. 12. Computed and measured values of β/k_0 for the $o\mathrm{HE}_{21}$ and $e\mathrm{HE}_{21}$ modes.

ductor plates and resonance frequencies from 8 to 12 GHz were measured by using a microwave counter. Measured guide wavelength and free-space wavelength were arranged to give the values of β/k_0. The measured values of β/k_0 are compared with the computed values of β/k_0 for various modes as shown in Figs. 10, 11, and 12.

V. Conclusion

Good agreement between the measured and computed values of β/k_0 is seen in Figs. 10, 11, and 12, which encourages us to adopt the point-matching method in analyzing other composite dielectric waveguides. A unique feature of these waveguides such as the separation of the polarization degeneracy could be also used in millimeter-wave or optical fiber applications. Complicated multi-core fiber structures, which have recently been proposed, could also be analyzed by applying this analytical method to a simplified model as shown in Fig. 1 (d).

Acknowledgment

The authors are grateful for the cooperation of the Optical Transmission Line Facility Section, Ibaraki electrical Communication Laboratory, NTT.

References

[1] D. Hondros and P. Debye, "Elektromagnetische Wellen an dielektrischen Drahten," *Ann. d. Phys.*, vol. 32, p. 465, June 1910.

[2] R. M. Knox, "Dielectric waveguide microwave integrated circuits: an overview," *IEEE Trans. Microwave Theory Tech.*, vol. MTT-24, pp. 806–814, Nov. 1976.

[3] D. Gloge, Ed., *Optical Fiber Technology*. New York: IEEE Press, 1975.

[4] E. Yamashita, K. Atsuki, O. Hashimoto, and K. Kamijo, "Modal analysis of homogeneous optical fibers with deformed boundaries," *IEEE Trans. Microwave Theory Tech.*, vol. MTT-27, pp. 352–356, Apr. 1979.

[5] V. Ramaswamy, I. P. Kaminow, and P. Kaiser, "Single polarization optical fibers: Exposed cladding techniques," *Appl. Phys. Lett.*, vol. 33, no. 9, pp. 814–816, Nov. 1978.

[6] J. E. Goell, "A circular-harmonic computer analysis of rectangular dielectric waveguides," *Bell Syst. Tech. J.*, vol. 48, pp. 2133–2160, Sept. 1969.